Synthesis and Characterization of Magnetic $CoFe_{1.9}Cr_{0.1}O_4$ Nanoparticles by Sol-gel Method and Their Applications as an Adsorbent for Water Treatment

Ibrahim A. Amar[1*], Abubaker Sharif[2] , Najat A. Omer[3], Naght E. Akale[4], Fatima Altohami[5], Mabroukah A. AbdulQadir[6]

[1]ibr.amar@sebhau.edu.ly, [2]abu.sharif@sebhau.edu.ly, [3]njat.abdalhfed@fsc.sebhau.edu.ly,
[4]naja.algali@fsc.sebhau.edu.ly, [5]fat.altohami@sebhau.edu.ly, [6]mabr.alsalheen@fsc.sebhau.edu.ly

[1-6] Department of Chemistry, Faculty of Sciences, Sebha University, Sebha/Libya
*Corresponding author email: ibr.amar@sebhau.edu.ly
Received: 00 April 2018 / Accepted: 00 May 2018

ABSTRACT

Water contamination by synthetic dyes is considered as a serious environmental issue, globally. In this study, the adsorptive removal of a very toxic cationic dye, methylene blue (MB), from aqueous solution was investigated using spinel ferrite, $CoFe_{1.9}Cr_{0.1}O_4$ (CFC), magnetic nanoparticles as an adsorbent. $CoFe_{1.9}Cr_{0.1}O_4$ powder was successfully synthesized via a sol-gel process and characterized by X-ray powder diffraction (XRD), Fourier transform infrared spectroscopy (FTIR) and scanning electron microscope (SEM) techniques. The effect of various experimental parameters on MB removal including; contact time, initial dye concentration, adsorbent dosage, solution pH and temperature were investigated. The results revealed that about 94 % of MB was removed under the optimal operational conditions. The adsorption kinetics showed that adsorption data were better described by pseudo-second-order model (PSO). In addition, the adsorption isotherms follow Langmuir isotherm model and the maximum monolayer adsorption capacity was found to be 11.41 mg/g. The calculated thermodynamic parameters (i.e., ΔG^o, ΔH^o, ΔS^o) indicate that the proposed adsorption process of methylene blue onto $CoFe_{1.9}Cr_{0.1}O_4$ nanoparticles is exothermic and spontaneous in nature. The results suggest that the synthesized magnetic nanoparticles (CFC) can be employed for the removal of toxic cationic synthetic dyes from wastewater.

Keywords: Spinel ferrites, adsorption, magnetic nanomaterials, methylene blue removal, nanotechnology, water purification.

1 Introduction

Water contamination by synthetic dyes has become a serious worldwide environmental issue owing to their adverse effect to human beings and aquatic life [1]. Dyes are important class of materials that have been widely used as coloring agents in many industries (e.g., paper, textile, cosmetics, etc.) [2]. Most of organic dyes which are discharged into the environment are toxic, mutagenic and carcinogenic in nature [3, 4]. Methylene blue (MB), a cationic dye, has found widespread use in textile industry [2]. The exposure to MB can cause a various type of health problems including; vomiting, nausea, profuse sweating, increased heart rate, mental confusion, quadriplegia, jaundice and cyanosis, etc. [2, 5]. Thus removal of this very toxic dye before getting discharged into water body is of crucial importance.

Adsorption is among different techniques (e.g., coagulation-flocculation, oxidation, membrane filtration, ion-exchange, photocatalytic degradation and biological treatment) that have been developed with the aim of treating dye-contaminated water. Adsorption is preferred due to its remarkable advantages such as; availability of various adsorbent types, ease of operation, low cost, simplicity of design, high removal efficiency and insensitivity to toxic pollutants, etc. [5-8].

Recently, magnetic nanoparticles (MNPs) have attracted considerable attention as adsorbent materials for the devolvement of next generation water treatment technology [9, 10]. Nanotechnology offers a great potential not only in advancing the current water treatment technologies, but also in providing a secure and sustainable water supply approach [11]. Among

MNPs adsorbents, spinel ferrites (MFe_2O_4, M = Co, Mg, Mn, Zn, etc.) are considered as promising adsorbent materials owing to their large specific surface area, fast kinetics, ease of functionalization, moderate saturation magnetization, ease of separation from water in the presence of external magnetic field, and thermal, chemical and mechanical stabilities, etc. [9, 10, 12]. Therefore, various spinel ferrites and their composites including; $MnFe_2O_4$ [13], $NiFe_2O_4$ [14], $Mn_{0.2}Zn_{0.8}Fe_2O_4$ [15], XFe_2O_4/GO (X = Co, Mn, Ni) [16] and AC/$Mn_{0.6}Zn_{0.4}Fe_2O_4$ [8] have been used as nano-adsorbents for MB removal from aqueous solutions. Recently, Reddy et al. [9] and Kefeni et al. [4] have reviewed the recent advances in the application of spinel ferrites nanoparticles (SFNPs) in the field of water purification. To the best of our knowledge, there is no report on using $CoFe_{1.9}Cr_{0.1}O_4$ (CFC) nanoparticles as adsorbent for the adsorptive removal of MB. Thus, the aim of the present work is to synthesise CFC nanoparticle and investigating its adsorption properties for MB removal from aqueous solutions.

2 Materials and Methods

2.1 Materials

Methylene blue dye (319.85 g/mol) was purchased from ScP (Surechem products). Cobalt nitrate ($Co(NO_3)_2{\cdot}6H_2O$) was purchased from Analyticals, Iron nitrate nonahydrate ($Fe(NO_3)_3{\cdot}9H_2O$) was purchased from Berck and Scientific Supplies. Chromium nitrate ($Cr(NO_2)_3.9H_2O$) was purchased from Farmitalia Carloerba-SPA. Citric acid ($C_6H_8O_7$) was purchased from Labkem. Ethylenediaminetetraacetic acid, EDTA, ($C_{10}H_{18}N_2O_8$) was purchased from Serva. Hydrochloric acid (HCl) was purchased from BDH Chemicals. Sodium hydroxide (NaCl) was purchased from Fluka. Amonia was purchased from Scharlau. All chemical were used as received without further purification.

2.2 Synthesis of $CoFe_{1.9}Cr_{0.1}O_4$ Nanoparticles

$CoFe_{1.9}Cr_{0.1}O_4$ (CFC) magnetic nanoparticles were synthesized using sol-gel method [17]. Briefly, $Co(NO_3)_2{\cdot}6H_2O$, $Fe(NO_3)_3{\cdot}9H_2O$ and $Cr(NO_2)_3.9H_2O$ were used as starting materials. Calculated amounts of these materials were dissolved in deionized water. Then, citric acid and EDTA were added to the mixed solution before adjusting its pH value to around 6 using ammonia solution. The mixed solution was evaporated to dryness and the resulted solid product was calcined in air at 600 °C for 3 h to obtain CFC powder.

2.3 Characterization of $CoFe_{1.9}Mo_{0.1}O_4$ Nanoparticles

XRD analysis was carried out using a Philips – PW 1800 diffractometer with CuKα radiation (λ=1.54186 Å). The sample was scanned over 2θ ranging from 1.4 to 79.4º, with a step size of 0.02º. Equations (1) and (2) were used to estimate the average particle size (D) and lattice parameters (a) of CFC nanoparticles [18].

$$D = \frac{0.9\,\lambda}{(\beta\cos\theta)} \quad (1)$$

$$d_{hkl} = \frac{\lambda}{2sin\theta} \quad ; \quad a = d_{hkl}\sqrt{h^2 + k^2 + l^2} \quad (2)$$

Where λ is the wavelength of the X-ray, θ is the Bragg angle, β is the full width at half maximum (FWHM) of the peak in radiance, d is the interplanar distance and hkl are the Miller indices.

Fourier transform infrared spectrum (FTIR) was collected in the region of 400 to 4000 cm^{-1}, in KBr pellets, using a Bruker Tensor 27 spectrophotometer. The surface morphology of CFC nanoparticles was investigated by scanning electron microscopy (SEM) using a LEO 1430PV instrument. Typical "drift method" was used to determine the pH of CFC nanoparticles at the point of zero charge (pH_{PZC}) using NaCl solution (0.1 mol/L) [19]. Then, 25 mL of NaCl was transferred to a series flasks and the initial pH value (pH_i) was adjusted to 3, 5, 7, 9 and 11 by adding either a 0.1 mol/L solution of HCl or NaOH. To each flask, 0.1 g of CFC nanoparticles was added and the flasks were closed tightly. After a shaking of 24 h, the final pH value (pH_f) was measured. The pH_{PZC} was obtained from the plot of ΔpH (pH_i -pH_f) against the pH_i [20]. All experiments were carried out at room temperature (~ 25 °C), otherwise stated.

2.4 Adsorption Experiments

A stock solution of MB (500 mg/L) was prepared by dissolving the accurate amount of MB into deionized water. The desired concentration of MB was obtained by diluting the stock solution. The adsorption experiments were performed in batch mode by shaking the adsorbent (CFC) and 20 mL of MB solution in a closed 25 mL Erlenmeyer flask for a certain agitation time at speed of 320 rpm using an orbital shaker (IKA-Werke). The MB adsorption into CFC surface was investigated under different experimental conditions including; contact time (0-120 min), initial dye concentration (25-55 mg/L), adsorbent dosage (0.01-0.20 g/20 mL), initial pH (3-11), and solution temperature (25-55 ºC). A diluted solution of either HCl or NaOH at a concentration of 0.1 mol/L was used to adjust the pH of dye solution using a pH meter (Jenway model 3505). A single beam UV-vis spectrophotometer (Jenway model 6305) was used to determine the MB concentration before and after adsorption experiments at λ_{ma} of 662 nm [2]. The percentage of MB removal (*%R*), the amount of MB adsorbed at any time t (q_t, mg/g) and the amount of MB adsorbed at equilibrium (q_e, mg/g), are calculated using the following equations [3, 21]:

$$\%R = \frac{C_o - C_t}{C_o} \times 100 \quad (3)$$

$$q_t = \frac{V(C_o - C_t)}{m} \quad (4)$$

$$q_e = \frac{V(C_o - C_e)}{m} \quad (5)$$

where C_o is the initial dye concentrations (mg/L), C_t and C_e are the final dye concentration (mg/L) at any time t and at equilibrium, respectively. m is the adsorbent dosage (g) and V is the volume of dye solution (L). To minimize the experimental errors, the adsorption experiments were performed in triplicate and the data were reported as the mean ± SD.

3 Theory and Calculation

3.1 Adsorption Kinetics

In this study, two common kinetic models including; pseudo-first-order (PFO) [22] and pseudo-second-order (PSO) [23] were applied for better understanding the adsorption process kinetics. For this purpose, the experimental data were fitted to the linear forms of PFO (Equation (6)) and PSO (Equation (7)), as expressed below [24];

$$\ln(q_e - q_t) = \ln q_e - k_1 t \quad (6)$$

$$\frac{t}{q_t} = \frac{1}{k_2 q_e^2} + \frac{1}{q_e} t \quad (7)$$

where q_e and q_t are as stated above, k_1 is PFO constant (min^{-1}) and k_2 is PSO (g/mg min). The values of q_e and k_1 were calculated from the intercept and slope of the plot of $\ln(q_e - q_t)$ versus t, respectively. The values of k_2 and q_e and were calculated from the intercept and the slop of plot of t/q_t versus t.

3.2 Adsorption Isotherms

To describe the nature of adsorbate-adsorbent interaction, the two most widely used isotherm models namely Langmuir [25] and Freundlich [26] were employed. Therefore, the experimental data at varying initial dye concentrations (25-55 mg/L) were fitted using these isotherm models. Langmuir and Freundlich isotherm models are suitable for describing the adsorption on homogenous and heterogeneous surfaces, respectively. The linearized forms of Langmuir and Freundlich isotherms can be expressed using Equations (8) and (9), respectively, as described below [24];

$$\frac{C_e}{q_e} = \frac{1}{q_{\max} K_L} + \frac{1}{q_{\max}} \quad (8)$$

$$\ln q_e = \ln K_F + \frac{1}{n} \ln C_e \quad (9)$$

where $q_{\max}$ is the maximum amount of MB adsorbed (mg/g), K_L and K_F are Langmuir (L/mg) and Freundlich ((mg/g)/(mg/L)^n) constants, respectively. n is Freundlich intensity parameter (dimensionless), which indicates the surface heterogeneity or the adsorption driving force. The adsorption isotherm is favourable $(n < 1)$, unfavourable $(n > 1)$, irreversible $(n = 0)$ and linear $(n = 1)$. The values of $q_{\max}$ and K_L, respectively, were calculated from the slope $(1/q_{\max})$ and the intercept $(1/q_{\max} K_L)$ of the linear plot of C_e against $C_e/q_{\max}$. The values of n and K_F, respectively, were calculated from the slope $(1/n)$ and the intercept $(\ln K_F)$ of the linear plot of $\ln C_e$ against $\ln q_e$. The feasibility of adsorption process can be evaluated using a dimensionless constant related to Langmuir isotherm called separation factor (R_L). The R_L value can be determined using the following equation [24].

$$R_L = \frac{1}{1 + K_L C_e} \tag{10}$$

The value of R_L suggests the type of the isotherm as follows; unfavourable $(R_L > 1)$, favourable $(0 < R_L < 1)$, irreversible $(R_L = 0)$ and linear $(R_L = 1)$.

3.3 Adsorption Thermodynamics

The thermodynamic parameters including Gibb's free energy change (ΔG^o), enthalpy change (ΔH^o) and entropy change (ΔS^o) were calculated using the following equations [24, 27];

$$\Delta G^o = \Delta H^o - T\Delta S^o \tag{11}$$

$$\ln K_c = \frac{-\Delta H^o}{R}\frac{1}{T} + \frac{\Delta S^o}{R} \tag{12}$$

$$K_c = \frac{C_s}{C_e} \tag{13}$$

where K_c is the distribution coefficient which calculated using Equation (13), C_s is the dye concentration on the adsorbent surface (mg/L), R is the gas constant (8.314 J/mol/K) and T is absolute temperature (K). The values of ΔH^o (kJ/mol) and ΔS^o (kJ/mol) were determined from the slope and the intercept of the plot of $\ln K_c$ versus $(1/T)$, respectively.

4 Results and Discussion

4.1 Characterization of $CoFe_{1.9}Cr_{0.1}O_4$ Adsorbent

Figure 1 shows the characteristic of $CoFe_{1.9}Cr_{0.1}O_4$ (CFC) magnetic nanoparticles. The XRD patterns of CFC calcined in air at 600 °C for 3 h are shown in Figure 1(a). The result indicates that a single phase of spinel ferrite (CFC) was obtained and all the diffraction peaks in XRD pattern are well indexed to the cubic structure of magnetite (JCPDS card No. 19-0629). The average crystallite size (*D*), lattice parameters (*a*) and the unit cell volume (a^3) of CFC adsorbent were found to be 38.63 nm, 8.3160 ± 0.0996 Å and 575.29 (Å)^3, respectively. The FTIR spectrum of CFC nanoparticles is presented in Figure 1(b). As shown, the typical characteristic peak for all spinel oxides which corresponds to metal-oxygen vibration (Fe-O) was observed at 586 cm^{-1}. The absorption peaks within the range of 874 to 1129 cm^{-1} are assigned to NO_3^- group that trapped during the synthesis of CFC nanoparticles. The observed peaks at approximately 1626 and 3402 cm^{-1} were attributed to O-H bending vibrations and O-H stretching vibrations, respectively [21, 28, 29]. Figure 1 (c) represents the SEM image of CFC magnetic nanoparticles which shows a heterogeneous structure with many pores. These pores are expected to enhance the adsorption properties of CFC nanoparticles. Figure 1(d) shows the pH at the point of zero charge (pH_{PZC}) of CFC nanoparticles. As can be seen, the pH_{PZC} value of CFC nanoparticles was equal to 6.33.

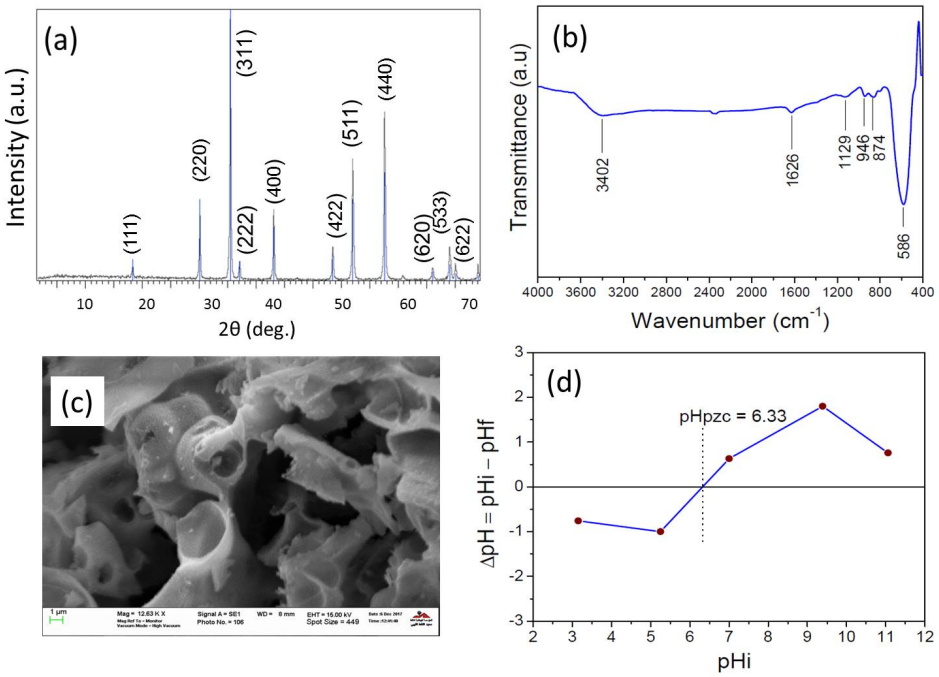

Figure 1: *(a) XRD pattern, (b) FTIR spectrum, (C) SEM and (d) the point of zero charge of CFC magnetic nanoparticle*

4.2 Adsorption Study

4.2.1 Effect of Contact Time

Figure 2 shows the effect of the contact time on the removal percentage (%R) of MB. In this experiment, 25 mg/L, 60 min and 0.01 g/20 mL were used as the initial MB concentration, contact time and adsorbent dosage, respectively. As can be seen, the %R increased significantly with increasing the contact time. In addition, a value of about 69.79% was attained when the contact time reached a 60 min after which no significant change in the %R was observed. This could be due to the saturation of the available active sites onto the adsorbent [30]. Thus, 60 min seems to be the optimum contact time.

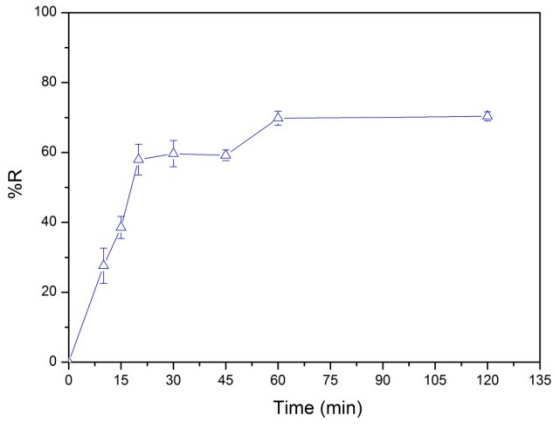

Figure 2: *Effect of the contact time on the percent removal of MB*

4.2.2 Effect of the initial dye concentration

The effect of MB dye concentration on the %R was investigated by varying the initial MB concentration from 25 to 55 mg/L and keeping the other operational condition at constant values (contact time of 60 min, adsorbent dosage of 0.01g/20 mL and room temperature. As shown from Figure 3, there is significant decrease in the %R value from 69.79% to

22.85% with increasing the MB concentration from 25 to 55 mg/L. This decrease in the percentage removal of MB could be due to the saturation the active adsorption sites of the adsorbent nanoparticles (CFC) after adsorbing a certain amount of MB dye molecules [31]. Therefore 25 mg/L was chosen as an optimum concentration for further studies.

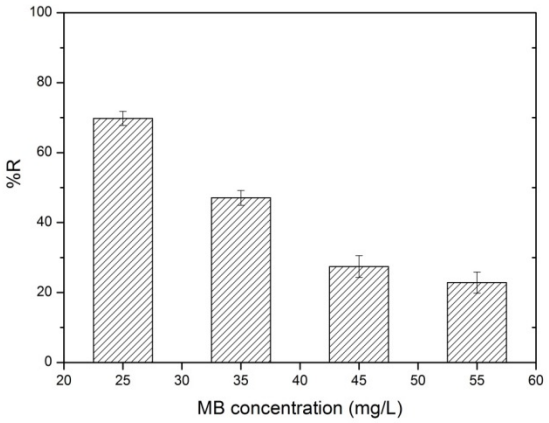

Figure 3: *Effect of the initial dye concentration on the MB removal percentage*

4.2.3 Effect of Adsorbent Dosage

The adsorption of MB (25 mg/L) using different adsorbent dosages (0.01-0.20 g/20 mL) is shown in Figure 4. The results reveal that the %R of MB increased from 45.92 to 69.97% by increasing the adsorbent dosage from 0.01 to 0.02 g/20 mL. This could be due to the increase in the number of active sites on the adsorbent surface [3]. However, no significant change in the %R was observed by future increasing the adsorbent dosage from 0.02 to 0.2 g/20 mL. Thus, 0.02 g/20 mL was chosen as the optimum adsorbent dosage. Figure 4 also shows that the amount of MB adsorbed at the equilibrium (q_e, mg/g) decreased significantly as the adsorbent dosage was increased 0.01 to 0.2 g/20 mL (22.96 to 1.83 mg/g). This may be due to the decrease in adsorbent total surface area as a result of aggregation or overlapping of the available active sites [2].

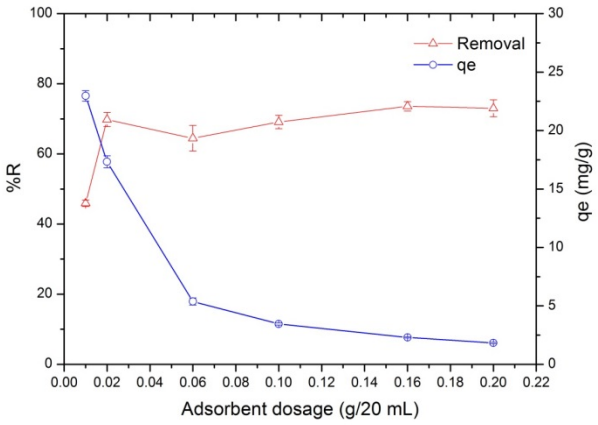

Figure 4: *Effect of the adsorbent dosage on the MB removal percentage and the amount of MB adsorbed at the equilibrium*

4.2.4 Effect of Solution pH

Figure 5 shows the effect of initial solution pH on the %R MB onto CFC nanoparticles. This effect was investigated by varying the initial pH of MB solution from 3 to 11 and keeping the other experimental condition at the optimized values. As shown, there is an increase in the %R value by increasing the solution pH from 3 to 5 (81.84 to 93.54%). However, the

%R value decreased as the solution pH was further increased. Therefore, a pH value of 5 was chosen as the optimum value. As mention above, the pH_{PZC} of CFC was found to be 6.33, suggesting that its surface will be positively charged below the pH_{PZC} and negatively charged above the pH_{PZC} [9]. MB is a cationic dye and gives positively charged ions in the aqueous solutions [32]. This means that the %R value should be high above 6.33 as the surface of CFC is negatively charged. In addition, MB molecules that contain Cl^- and NaOH that used for adjusting the pH values will undergo to replacement reaction and resulting in NaCl formation. Hence, the decreased %R values at high pH values (> 5) might be due to in the increase in the solution ionic strength that resulted from NaCl formation [33].

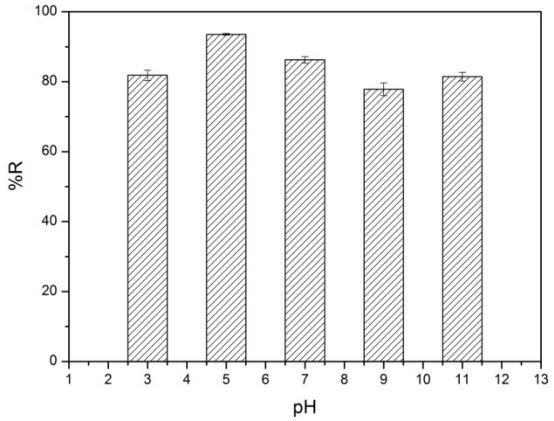

Figure 5: *Effect of initial pH on the MB removal percentage*

4.2.5 Effect of Solution Temperature

To investigate the effect of solution temperature on the %R of MB onto CFC nanoparticles, the experiment was carried out at different temperatures (25 to 55 °C) under the optimum operational conditions (contact time of 60 min, initial MB concentration of 25 mg/L and adsorbent dosage of 0.02 g/20 mL and pH value of 5). The results revealed that the %R decreased from 91.06 to 59.11% with increasing the solution temperature from 25 to 55 °C, as presented in Figure 6. This indicates that the proposed adsorption process is exothermic in nature. This decrease in the %R of MB with increasing solution temperature can be attributed the increase in the mobility of dye molecule. Consequently, less MB molecules were adsorbed onto CFC nanoparticles at high temperature [6].

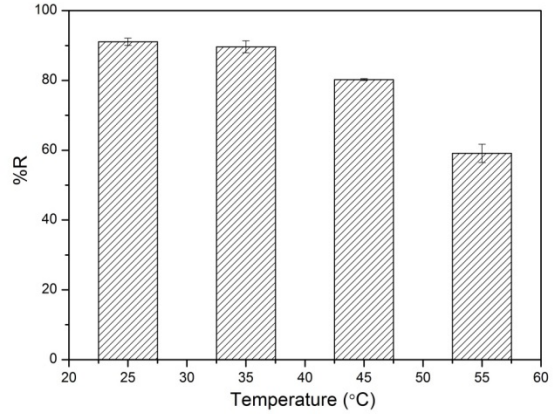

Figure 6: *Effect of solution temperature on the MB removal percentage*

4.3 Adsorption Kinetics

In the present study, pseudo-first-order (PFO) and pseudo-second-order (PSO) kinetic models were employed to evaluate the adsorption data using linear regression method. Table 1 lists the fitting parameters of these two models. As listed in the table, the calculated $q_{e,cal}$ value that obtained from PSO is close to the experimental $q_{e,exp}$ value, in contrast to the value obtained from PFO. In addition, the correlation coefficient (R^2) value of PSO was found to be 0.9759 which is higher than that of PFO (0.8208). This indicates that the pseudo-second-order model is more applicable for describing the adsorption kinetics of MB onto CFC nanoparticle.

Table 1: *Kinetic parameters for the adsorption of MB onto CFC nanoparticles*

$q_{e,exp}$ (mg/g)	Pseudo-first-order		
	$q_{e,cal}$ (mg/g)	k_1 (min^{-1})	R^2
17.73	20.63	7.01×10^{-2}	0.8208
	Pseudo-second-order		
	$q_{e,cal}$ (mg/g)	k_2 (g/mg.min)	R^2
	19.25	6.69×10^{-3}	0.9759

4.4 Adsorption Isotherms

Langmuir and Freundlich isotherm parameters such as $q_{\max}$, K_L, K_F, n and R^2 are listed in Table 2. According to the tabulated values, Langmuir isotherm model exhibits the highest correlation coefficient value $(R^2 = 0.9859)$. This means that the proposed adsorption process is better described by Langmuir isotherm. Furthermore, the maximum adsorbed amount of MB $(q_{\max})$ is found to be 11.41 mg/g. This value is higher than the value (3.31 mg/g) that reported by Patil et al. [34] for MB adsorption using an adsorbent composed of polyaniline-spinel ferrite (PANI-$NiFe_2O_4$) and lower than the value (40.97 mg/g) obtained using $Mn_{0.2}Zn_{0.8}Fe_2O_4$ as an adsorbent as reported by Hou et al. [15]. In addition, the calculated R_L values within the initial concentration range of 25-55 mg/L were less than unity (0.59-0.39), indicating the favourability of the adsorption of MB onto CFC nanoparticles [24].

Table 2: *Adsorption isotherm parameters for adsorption of MB onto CFC nanoparticles*

Langmuir isotherm		
q_{max} (mg/g)	K_L (L/mg)	R^2
11.41	0.109	0.9859
Freundlish isotherm		
K_F (mg/g)/(mg/L)^n	n	R^2
27.8	4.69	0.7455

4.5 Adsorption Thermodynamics

Table 3 summarizes the calculated thermodynamic parameters of MB adsorption on CFC nanoparticles. The negative values of ΔG^o at different solution temperatures (298-328 K) indicate the proposed adsorption process is feasible and spontaneous in nature. In addition, as the solution temperature increased, the negative ΔG^o values decreased, indicating that low temperature is favourable for MB adsorption. The negative ΔH^o value implies that MB adsorption is exothermic process in nature. Furthermore, the value of ΔS^o was negative, indicating the decreased randomness at the solid/liquid interface during the proposed process.

Table 3: *Thermodynamic parameters for adsorption of MB onto CFC nanoparticles*

ΔH^o (kJ/mol)	ΔS^o (J/mol.K)	ΔG^o (kJ/mol)			
		298 K	308 K	318 K	328 K
- 53.26	- 157.38	-6.36	-4.79	-3.21	-1.64

5 Conclusions

In summary, spinel ferrite, $CoFe_{1.9}Cr_{0.1}O_4$ (CFC), magnetic nanoparticles were successfully synthesized and employed as adsorbent for the removal of MB from aqueous solutions. The adsorption process was highly dependent on the operational conditions. More than 90% of MB was removed at the optimum conditions (i.e., contact time of 60 min, initial dye concentration of 25 mg/L, adsorbent dosage of 0.02 g/20 mL, initial solution pH of 5 and solution temperature of 25 °C. The kinetic study indicated the applicability of pseudo-second-order for describing the adsorption data. The isotherm study revealed that Langmuir isotherm better described the adsorption of MB onto CFC nanoparticles. The maximum adsorbed amount of MB was found to be 11.41 mg/g. The calculated thermodynamic parameters demonstrated that the proposed adsorption process was feasible, spontaneous and exothermic in nature. The results revealed that the prepared magnetic adsorbent (CFC) is a promising and can be employed for the removal of very toxic organic materials from wastewater.

6 Acknowledgment

The authors are thankful to the Department of Chemistry, Sebha University, Sebha, Libya for the financial support of this work. The authors also thank the Central Laboratory at Sebha University, Sebha Libya for providing the furnace for material calcination. The authors thank the Libyan Petroleum Institute, Tripoli, Libya for performing XRD and SEM analysis. The authors also thank Mr. Fathi Elsharif and Mr. Khaled Azzabi from the Nuclear Research Centre, Tajoura, Libya for performing FTIR analysis.

References

[1] C. Santhosh, V. Velmurugan, G. Jacob, S. K. Jeong, A. N. Grace and A. Bhatnagar "Role of nanomaterials in water treatment applications: A review," *Chemical Engineering Journal*, vol. 306, pp. 1116-1137, 2016.

[2] H. Singh, G. Chauhan, A. K. Jain and S. K. Sharma, "Adsorptive potential of agricultural wastes for removal of dyes from aqueous solutions," *Journal of Environmental Chemical Engineering*, vol. 5, pp. 122-135, 2017.

[3] F. Moeinpour, A. Alimoradi, and M. Kazemi, "Efficient removal of Eriochrome black-T from aqueous solution using $NiFe_2O_4$ magnetic nanoparticles," *Journal of Environmental Health Science and Engineering*, vol. 12, pp. 112, 2014.

[4] K. K. Kefeni, B. B. Mamba, and T. A. M. Msagati, "Application of spinel ferrite nanoparticles in water and wastewater treatment: A review," *Separation and Purification Technology*, vol. 188, pp. 399-422, 2017.

[5] M. Rafatullah, O. Sulaiman, R. Hashim and A. Ahmad, "Adsorption of methylene blue on low-cost adsorbents: A review," *Journal of Hazardous Materials*, vol. 177, no. 1-3, pp. 70-80, 2010.

[6] T. K. Mahto, A. R. Chowdhuri, and S. K. Sahu, "Polyaniline-functionalized magnetic nanoparticles for the removal of toxic dye from wastewater," *Journal of Applied Polymer Science*, vol. 131, pp. 40840, 2014.

[7] A. Ahmed, S. H. Mohd-Setapar, C. S. Chuon, A. Khatoon, W. A. Wani, R. Kumar and M. Rafatullah, "Recent advances in new generation dye removal technologies: noval search for approaches to repocess wastewater," *RSC Advances*, vol. 5, pp. 30801-30818, 2015.

[8] R. Wang, J. Yu, and Q. Hao, "Activated carbon/$Mn_{0.6}Zn_{0.4}Fe_2O_4$ composites: Facile synthesis, magnetic performance and their potential application for the removal of methylene blue from water," *Chemical Engineering Research and Design*, vol. 132, pp. 215-225, 2018.

[9] D. H. K. Reddy, and Y. S. Yun, "Spinel ferrite magnetic adsorbents: alternative future materials for water purification?," *Coordination Chemistry Reviews*, vol. 315, pp. 90-111, 2016.

[10] D. Mehta, S. Mazumdar, and S. K. Singh, "Magnetic adsorbents for the treatment of water/wastewater-A review," *Journal of Water Process Engineering*, vol. 7, pp. 244-265, 2015.

[11] Y. Zhang, B. Wu, H. Xu, H. Liu, Hui, M. Wang, Y. He and B. Pan, "Nanomaterials-enabled water and wastewater treatment," *NanoImpact*, vol. 3–4, pp. 22-39, 2016.

[12] J. Gomez-Pastora, E. Bringas, and I. Ortiz, "Recent progress and future challenges of high performance magnetic nano-adsorbent in environmental applications," *Chemical Engineering Journal*, vol. 256, pp. 187-204, 2014.

[13] X. Hou, J. Feng, Y. Ren, Z. Fan and M. Zhang, "Synthesis and adsorption properties of spongelike porous $MnFe_2O_4$," Colloids and Surfaces A: *Physicochemical and Engineering Aspects*, vol. 363, pp. 1-7, 2010.

[14] X. Hou, J. Feng, X. Liu, Y. Ren, Z. Fan, T. Wei, J. Meng and M. Zhang, "Synthesis of 3D porous ferromagnetic $NiFe_2O_4$ and using as novel adsorbent to treat wastewater," *Journal of colloid and interface science*, vol. 362, pp. 477-485, 2011.

[15] X. Hou, J. Feng, X. Liu, Y. Ren, Z. Fan and M. Zhang, "Magnetic and high rate adsorption properties of porous $Mn_{1-x}Zn_xFe_2O_4$ ($0 \leqslant x \leqslant 0.8$) adsorbents," *Journal of colloid and interface science*, vol. 353, pp. 524-529, 2011.

[16] L. G. Bach, T. V. Tran, T. D. Nguyen, T. V. Pham and S. T. Do, "Enhanced adsorption of methylene blue onto graphene oxide-doped XFe_2O_4 (X = Co, Mn, Ni) nanocomposites: kinetic, isothermal, thermodynamic and recyclability studies," *Research on Chemical Intermediates*, vol. 44, pp. 1661-1687, 2018.
[17] Y. Ling, J. Yu, B. Lin, X. Zhang, L. Zhao and X. Liu, "A cobalt-free $Sm_{0.5}Sr_{0.5}Fe_{0.8}Cu_{0.2}O_{3-\delta}$-$Ce_{0.8}Sm_{0.2}O_{2-\delta}$ composite cathode for proton-conducting solid oxide fuel cells," *Journal of Power Sources*, vol. 196, pp. 2631-2634, 2011.
[18] Y. P. Fu, S. H. Chen, and J. J. Huang, "Preparation and characterization of $Ce_{0.8}M_{0.2}O_{2-\delta}$ (M = Y, Gd, Sm, Nd, La) solid electrolyte materials for solid oxide fuel cells," *International Journal of Hydrogen Energy*, vol. 35, pp. 745-752, 2010.
[19] M. Kosmulski, Surface charging and points of zero charge: CRC press, 2009.
[20] H. N. Tran, Y. F. Wang, S. J. You and H. P. Chao, "Insights into the mechanism of cationic dye adsorption on activated charcoal: The importance of π–π interactions," *Process Safety and Environmental Protection*, vol. 107, pp. 168-180, 2017/04/01/, 2017.
[21] W. Konicki, D. Sibera, E. Mijowska, Z. Lendzion-Bieluń and U. Narkiewicz, "Equilibrium and kinetic studies on acid dye Acid Red 88 adsorption by magnetic $ZnFe_2O_4$ spinel ferrite nanoparticles," *Journal of colloid and interface science*, vol. 398, pp. 152-160, 2013.
[22] S. Lagergren, "About the Theory of so-called Adsorption of Soluble Substances," *Kungliga Sevenska Vetenskapasakademiens Handlingar*, vol. 24, pp. 1-39, 1898.
[23] Y. S. Ho, and G. McKay, "Pseudo-second order model for sorption processes," *Process Biochemistry*, vol. 34, pp. 451-465, 1999.
[24] H. N. Tran, S. J. You, A. Hosseini-Bandegharaei and H. P. Chao, "Mistakes and inconsistencies regarding adsorption of contaminants from aqueous solutions: A critical review," *Water Research*, vol. 120, pp. 88-116, 2017.
[25] I. Langmuir, "The constitution and fundamental properties of solids and liquids. Part I. Solids. ," *The Journal of the American Chemical Society*, vol. 38, pp. 2221-2295, 1916.
[26] H. M. F. Freundlich, "Over the adsorption in solution," *The Journal of Physical Chemistry*, vol. 57, pp. 385-470, 1906.
[27] L. R. Bonetto, F. Ferrarini, C. D. Marco, J. S. Crespo, R. Guégan and M. Giovanela, "Removal of methyl violet 2B dye from aqueous solution using a magnetic composite as an adsorbent," *Journal of Water Process Engineering*, vol. 6, pp. 11-20, 2015.
[28] M. Stoia, and C. Muntean, "Preparation, Characterization and Adsorption Properties of MFe_2O_4 (M = Ni, Co, Cu) Nanopowders," *Environmental Engineering and Managment Journal*, vol. 14, pp. 1247-1259, 2015.
[29] W. Wang, Z. Ding, M. Cai, H. Jian, Z. Zeng, F. Li and J. P. Liu, "Synthesis and high-efficiency methylene blue adsorption of magnetic PAA/$MnFe_2O_4$ nanocomposites," *Applied Surface Science*, vol. 346, pp. 348-353, 2015.
[30] K. Erol, K. Köse, D. A. Köse, U. Sızır, S. İ. Tosun and L. Uzun, "Adsorption of Victoria Blue R (VBR) dye on magnetic microparticles containing Fe (II)–Co (II) double salt," *Desalination and Water Treatment*, vol. 57, pp. 9307-9317, 2016.
[31] S. Chawla, H. Uppal, M. Yadav, N. Bahadur and N. Singh, "Zinc peroxide nanomaterial as an adsorbent for removal of Congo red dye from waste water," *Ecotoxicology and Environmental Safety*, vol. 135, pp. 68-74, 2017.
[32] M. F. Zayed, W. H. Eisa, and B. Anis, "Removal of methylene blue using Phoenix dactylifera/PVA composite; an eco-friendly adsorbent," *Desalination and Water Treatment*, vol. 57, pp. 18861-18867, 2016.
[33] Z. A. Al-Anber, M. A. Al-Anber, M. Matouq, O. Al-Ayed and N. M. Omari, "Defatted Jojoba for the removal of methylene blue from aqueous solution: Thermodynamic and kinetic studies," *Desalination*, vol. 276, pp. 169-174, 2011.
[34] M. R. Patil, and V. Shrivastava, "Adsorptive removal of methylene blue from aqueous solution by polyaniline-nickel ferrite nanocomposite: a kinetic approach," *Desalination and Water Treatment*, vol. 57, pp. 5879-5887, 2016.